19th Brazilian Congress of Thermal Sciences and Engineering
November 06th-10th, 2022, Bento Gonçalves - RS - Brazil

ENC-2022-0073
NUMERICAL INVESTIGATION ON THE THERMAL BEHAVIOR OF A TURBOGENERATOR

Felipe Augusto Menon
Guilherme Schneider Porepp
WEG S.A. – Av. Pref. Waldemar Grubba, 3000 – 89256-900 – Jaraguá do Sul, SC, Brazil
e-felipeam@weg.net, guilhermesp@weg.net

Abstract. *In this paper, a turbogenerator was numerically studied with a focus on the thermal behavior of the rotor. For this purpose, a three-dimensional model was developed. The governing equations (i.e., conservation of mass, momentum and energy) were solved with commercial software Ansys CFX, which employs the finite volume method. The results are shown to be in good agreement with experimental data. Predicted windage losses amounted to 243.5 kW, presenting an error of 1.5% in comparison with the measured value. The average temperature rise of the rotor windings was estimated to be 90.7 ºC, with a relative error of less than 4%.*

Keywords: *Turbogenerator, Computational Fluid Dynamics (CFD), Thermal Analysis*

1. INTRODUCTION

A turbogenerator (or alternator) is a device designed to be connected to the shaft of a gas or steam turbine for the generation of electric power through the principle of electromagnetic induction. This technology is widely used in the energy industry. In fact, most of the world electricity is produced in such equipment (IEA, 2021).

During operation, heat is generated inside the alternator as a result of electromagnetic losses, causing its temperature to rise. Continuously high temperatures on generator windings could cause the degradation of its electrical insulation materials, shortening the life cycle of the product. It is therefore important to control the heating of these machines. In synchronous generators, this is mostly done by means of convective heat transfer.

Although essential to the integrity of the equipment, convective cooling introduces air flow losses that may account for up to 30% of the total power loss of an alternator. Thus, in order to obtain a low and uniform temperature distribution while trying to keep mechanical losses at a minimum, careful analysis is imperative at the design stage of the machine.

Conventionally, temperatures in electric generators are evaluated through analytical calculation, with the structuring and solution of equivalent hydraulic and thermal circuits. Despite being long established, this methodology has certain limitations when more detailed results are needed. Furthermore, it relies greatly on empirical correlations to estimate important parameters, such as pressure drop and convective heat transfer coefficients.

More recently, Computational Fluid Dynamics (CFD) proved to be an important tool in the design and development of alternators. Many papers have been published on the application of the finite volume method to the study of these machines, as it allows the computation of pressure, velocity and temperature fields and facilitates the prediction of frictional losses.

In the work of Hosain et al. (2017), for example, CFD was employed to analyze fluid flow and heat transfer within the air gap between the rotor and the stator. The simulation was able to capture complex Taylor vortices that could not be resolved with other modelling approaches.

Bersch et al. (2017) conducted an optimization study with the objective of minimizing the peak temperature of a generator. Varying the position of a radial channel in the stator core, the authors found that the optimal arrangement reduced the maximum temperature by 9.4 ºC. The analyses were carried out in Ansys Fluent.

Jichao et al. (2021) studied a 250 MW hydrogenator, numerically calculating the electromagnetic and thermal processes occurring inside the equipment. Estimated temperature for the rotor winding showed good agreement with measured values. On the occasion, a sensitivity analysis was also done in order to assess the influence of various rotor components.

In a similar manner, this work presents the numerical study of a turbogenerator focusing the thermal behavior of the rotor. Simulation results are discussed and compared with experimental data.

2. EQUIPMENT DESCRIPTION

The turbogenerator under study has four poles. To supply electricity at 60 Hz, a rotor speed of 1800 RPM is adopted. Constructive characteristics of the equipment can be seen in Fig. 1.

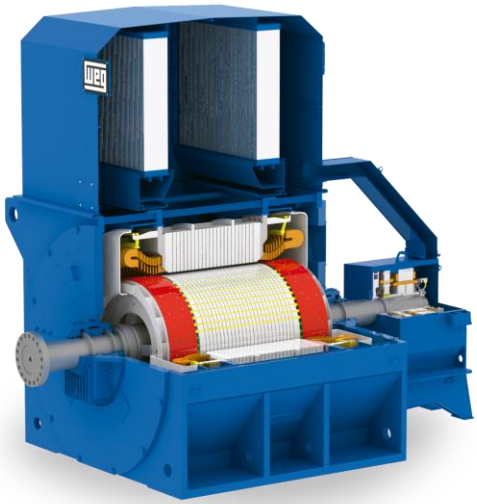

Figure 1. Section view of the turbogenerator.
Source: WEG S.A.

The active part of the machine is based on two main components: the stationary part, called the stator, and the rotating part, called the rotor. The stator consists of an assembly of annular-shaped silicon steel sheets, in which copper coils are positioned within a series of slots. The rotor core, mounted on the shaft, is also composed of a set of steel sheets, with a number copper coils being housed near its outer circumference.

The cooling system of the turbogenerator in question is that of a totally enclosed machine in which air is internally recirculated and cooled by an air-to-water heat exchanger. The concept is illustrated in Fig. 2.

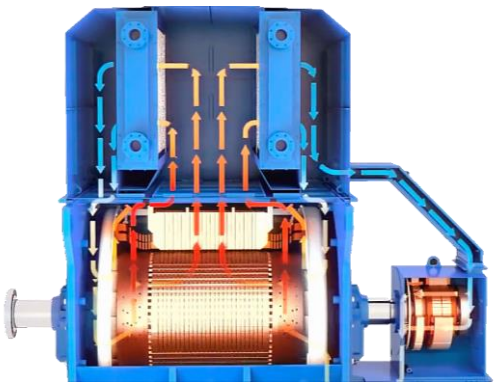

Figure 2. Turbogenerator cooling system.
Source: WEG S.A.

The internal ventilation is provided by two centrifugal fans with backward-curved blades, which are mounted directly on the shaft in a bilateral scheme. Air enters the rotor core axially. To ensure proper distribution, radial channels are employed both in the rotor and the stator.

3. COMPUTATIONAL FLUID DYNAMICS (CFD) MODELLING

The numerical simulations were performed with commercial software Ansys CFX, which employs the finite volume method in order to solve the governing equations over the whole domain.

3.1 Domains

From a modelling point of view, the study domain is divided into two groups: fluid domains and solid domains. Figure 3 presents both of them.

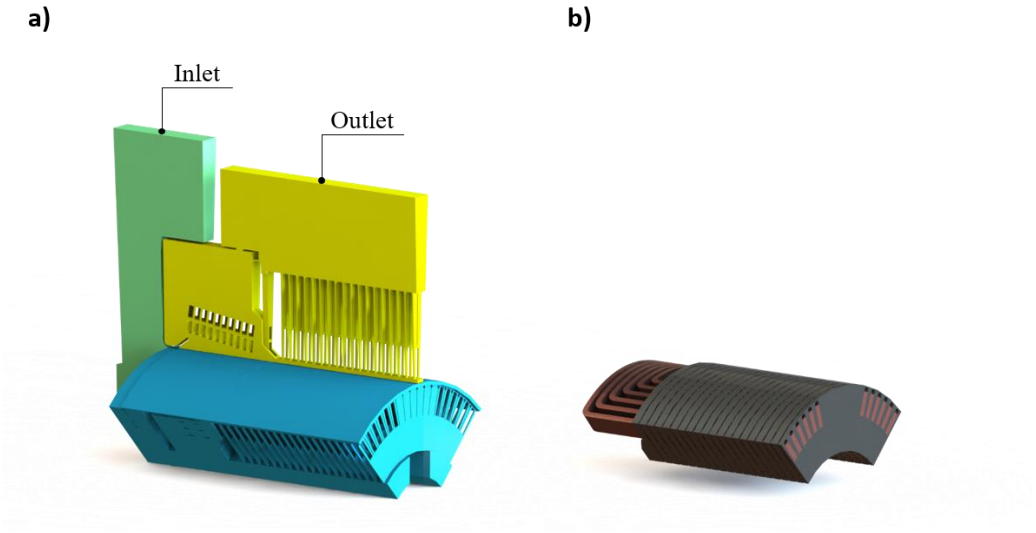

Figure 3. Study domains: a) fluid; and b) solid.

Fluid domains comprise the air in the inlet (green), rotor (blue) and stator (yellow) regions. As the main focus of this work was to analyze the thermal behavior of the rotor, only its solid parts were taken into account.

In order to reduce the computational costs associated with the simulation, each region was limited to its smallest representative volume. For the rotor, that is a 90º half slice. In other regions, slices of approximately 4º were adopted. Rotational periodicity and symmetry boundary conditions were then employed.

Inlet conditions were defined analytically. Pressure at the outlet was defined taking into consideration the loss promoted by the heat exchanger.

Spatial discretization was performed with Ansys Meshing. The generated mesh consists of 22438373 elements, being mostly tetrahedral. Prismatic elements were allocated near the walls to better capture boundary layer effects.

3.2 Governing equations

For fluid domains, the equations solved are, basically, the Reynolds averaged form of the conservation of mass, momentum and energy, given by Eq. (1), Eq. (2) and Eq. (3), respectively.

$$\frac{\partial \rho}{\partial t} + \frac{\partial}{\partial x_j}\left(\rho U_j\right) = 0 \tag{1}$$

$$\frac{\partial \rho U_i}{\partial t} + \frac{\partial}{\partial x_j}\left(\rho U_i U_j\right) = -\frac{\partial p'}{\partial x_i} + \frac{\partial}{\partial x_j}\left[\left(\mu + \mu_t\right)\left(\frac{\partial U_i}{\partial x_j} + \frac{\partial U_j}{\partial x_i}\right)\right] + S_M \tag{2}$$

$$\frac{\partial \rho h_{tot}}{\partial t} - \frac{\partial p}{\partial t} + \frac{\partial}{\partial x_j}\left(\rho U_j h_{tot}\right) = \frac{\partial}{\partial x_j}\left(\lambda \frac{\partial T}{\partial x_j} + \frac{\mu_t}{Pr_t}\frac{\partial h_{tot}}{\partial x_j}\right) + \frac{\partial}{\partial x_j}\left[U_i\left(\tau_{ij} - \overline{\rho u_i u_j}\right)\right] + S_E \tag{3}$$

As presented above, μ_t is the turbulent viscosity, Pr_t is the turbulent Prandtl number, h_{tot} is the mean total enthalpy and p' is a modified pressure term. All these variables are directly related to eddy viscosity models for turbulence.

Given the angular velocity of the rotor, the flow in this domain is subjected to Coriolis force, centrifugal force and angular acceleration. To account for these effects, source terms are included in the momentum (S_M) and energy (S_E) equations. Furthermore, the stagnation enthalpy is used in place of the total enthalpy. In other places, where there is no rotation, these terms are neglected.

In addition to Eq. (1), Eq. (2) and Eq. (3), partial differential equations describing the conservation of the turbulence kinetic energy (k) and turbulent frequency (ω) are also solved. The turbulence model employed in this study is the SST model. In short, it combines the k-ω and k-ε models, using the former for near-surface regions and the latter for regions

outside the boundary layer, while also taking the transport of turbulent shear stress into consideration. Mathematical formulation for the turbulence model is here omitted.

Finally, air is treated as an ideal gas. Therefore, ρ is calculated from the Ideal Gas Law and C_p is approximated as a function of temperature.

For solid domains, the conservation of energy is solved:

$$\frac{\partial \rho h}{\partial t} = \nabla \cdot (\lambda \nabla T) + S_E \tag{4}$$

where the source term S_E refers to the rate of internal heat generation per unit volume. It encompasses copper and iron losses, which were calculated in an external commercial software.

4. EXPERIMENTAL EVALUATION

It is quite difficult to perform tests at full load on large synchronous machines, as this requires extremely expensive and complex laboratory facilities. Therefore, in order to experimentally evaluate the temperature rise of the generator, an equivalent method had to be used. In accordance with IEC 60034-29, tests at reduced power were performed to determine the linear relationship between voltage (IR_2) and temperature rise (ΔT) in the rotor windings. Subsequently, this IR_2 vs. ΔT curve was extrapolated to obtain the temperature associated with the nominal Joule losses of the rotor.

In this study, the experimental curve was constructed with the short-circuit test and the no-load test. For both tests, the generator is driven by an electric motor and set to operate at its synchronous speed. In the short-circuit test, the stator terminals are connected. The field current is then gradually increased until the rated stator current is obtained. In the no-load test, in turn, the stator terminals are disconnected and kept open, so that there is no current in the component. The field current is increased until the rated stator voltage is obtained.

As the relation between IR_2 and ΔT must be linear, two points would be enough to determine the temperature of the rotor winding with rated loads. However, in order to minimize errors, it is recommended to adopt a third reference point, which can be obtained by tests similar to those mentioned above but under different current conditions. One could, for example, increase the rotor excitation during the short-circuit test or the no-load test, resulting in higher stator currents or voltages. Another possibility for obtaining this additional point is to resort to the zero power factor test.

Figure 4 shows the manufactured turbogenerator at the test facility.

Figure 4. Manufactured turbogenerator.
Source: WEG S.A.

Following the described methodology, an average temperature rise of 87.3 ºC was found for the rotor winding under rated conditions. Windage losses were measured to be 240.6 kW.

5. RESULTS

Figure 5 presents velocity, turbulence kinetic energy and temperature distributions for the air in a longitudinal plane of the rotor. Figure 6 shows contours of velocity, turbulence kinetic energy and static pressure in a transversal plane of the centrifugal fan. It is important to highlight that, while in Fig. 5 velocity results are relative to the rotating frame of reference, in Fig. 6 values are based on the stationary coordinate system.

Air flow rate inside the machine was estimated at 27.9 kg/s. The highest velocity, 116.3 m/s, was found to occur in the rotor region. Predicted windage losses amounted to 243.5 kW, an error of 1.5% in relation to the measured value.

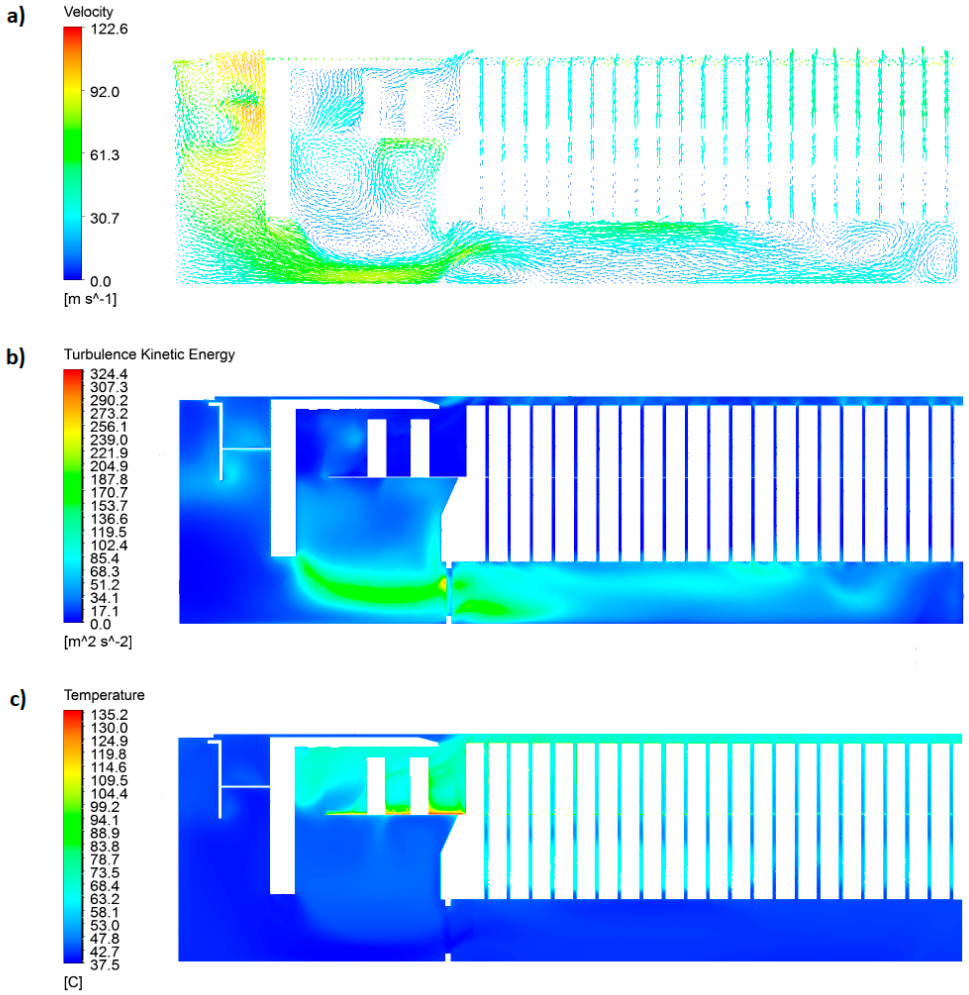

Figure 5. Results in a longitudinal plane of the rotor: a) velocity field; b) turbulence kinetic energy contours; and c) temperature contours.

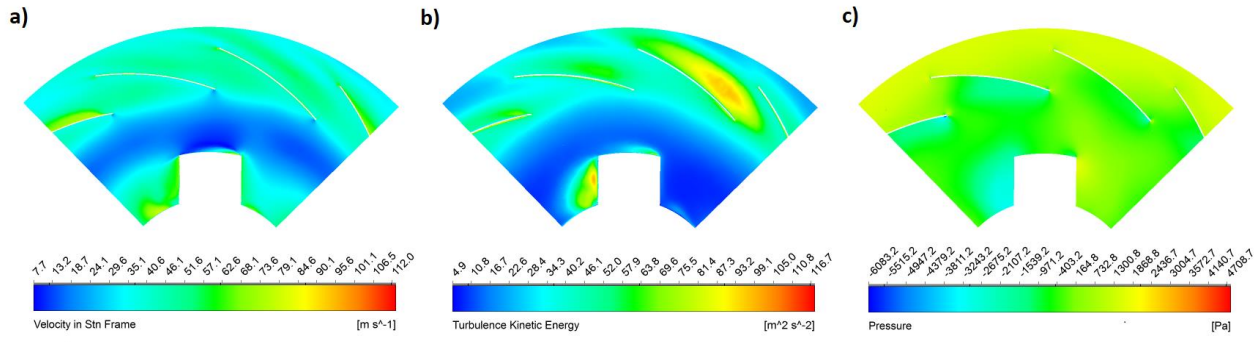

Figure 6. Results in a transversal plane of the fan: a) velocity contours; b) turbulence kinetic energy contours; and c) pressure contours.

Interestingly, one can visualize the wake turbulence generated by the fan blades during its rotation movement.

In Fig. 7, temperature distributions for the solid components of the rotor are shown. The average temperature rise of the windings was calculated to be 90.7 ºC, presenting a relative error of 3.9% in comparison with the experimentally

estimated value. An average temperature of 78.1 ºC was predicted for the core, with higher values at the ends and lower ones towards the center.

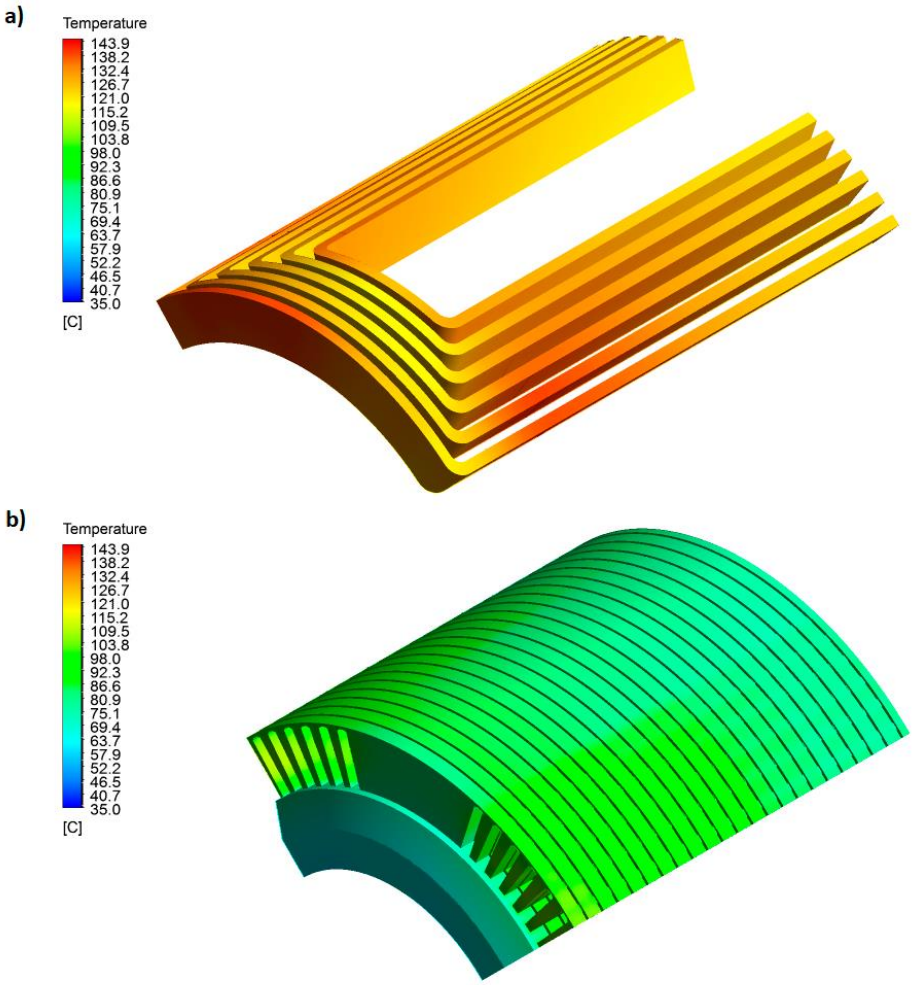

Figure 7. Temperature distribution of the rotor: a) windings; and b) core.

6. CONCLUSIONS

In this paper, Computational Fluid Dynamics was applied to the study of a turbogenerator with a greater focus on the thermal behavior of the rotor. Both complex flow inside the machine and conjugate heat transfer between solid and fluid domains were resolved. The simulation results proved to be quite reliable. Errors of 1.5% and 3.9% were found for the windage losses and the average temperature rise in the rotor windings. Overall, the study helps to emphasize the importance of numerical tools in the analysis of large rotating electrical machines.

7. ACKNOWLEDGEMENTS

The authors would like to thank Inova Talentos Program, a partnership between Euvaldo Lodi Institute (IEL, Brazil) and the National Council for Scientific and Technological Development (CNPq, Brazil), as well as WEG S.A. – Energy Unit (Brazil).

8. REFERENCES

Bersch, K., Connor, P.H., Eastwick, C.N., Galea, M. and Rolston, R., 2017. “CFD Optimisation of the Thermal Design for a Vented Electrical Machine”. In *Proceedings of the 2017 IEEE Workshop on Electrical Machines Design, Control and Diagnosis - WEMDCD 2017*. Nottingham, UK.

Hosain, M.L. and Fdhila, R.B., 2017. “Air-Gap Heat Transfer in Rotating Electrical Machines: A Parametric Study”. In *Proceedings of the 9th International Conference on Applied Energy - ICAE 2017*. Cardiff, UK.

IEA, 2021. “Electricity Information: Overview” International Energy Agency. 11 Jun. 2022 <www.iea.org>.

IEC, 2008. “IEC 60034-29 - Rotating Electrical Machines - Part 29: Equivalent loading and superposition techniques - Indirect testing to determine temperature rise” International Electrotechnical Commission.

Jichao, H., Yutian, S., Ping, Z., Haiming, Q., Jiechen, D., Yufei, L., Chunli, Z., Baojun, G. and Weili, L., 2021. “Influence of Complex Fluid Flow on Temperature Distribution in the Rotor Region of Large Hydrogenerator Under the Rotor Rotation”. *IEEE Access*, Vol. 10, pp. 3252–3262.

9. RESPONSIBILITY NOTICE

The authors are the only responsible for the printed material included in this paper.